Fe and Cr K-edges EXAFS Study of Double Perovskite $(Sr_{2-x}Ca_x)FeMoO_6$ $(0 \le x \le 2.0)$ and Sr_2CrMO_6 (M = Mo, W) Systems

T. S. Chan[a] (詹丁山), R. S. Liu[a]* (劉如熹) and L.-Y. Jang[b] (張凌雲)
[a]*Department of Chemistry and Center for Nano Storage Research, National Taiwan University, Taipei 106, Taiwan, R.O.C.*
[b]*National Synchrotron Radiation Research Center, Hsinchu 300, Taiwan, R.O.C.*

The local structure of the double perovskite $(Sr_{2-x}Ca_x)FeMoO_6$ $(0 \le x \le 2.0)$ and Sr_2CrMO_6 (M = Mo, W) systems have been probed by extended X-ray absorption fine structure (EXAFS) spectroscopy at the Fe and Cr *K*-edges. We found Fe-O (ave) distance apparently decreases from 1.999 Å (x = 0) to 1.991 Å (x = 1.0) in $(Sr_{2-x}Ca_x)FeMoO_6$ (tetragonal structure). When x is increased further from 1.5 to 2.0, the Fe-O bond distance decreased from 2.034 Å to 2.012 Å (monoclinic structure). In addition, Cr-O, Sr-Cr, and Cr-Mo bond distances in Sr_2CrWO_6 are all slightly larger than the bond distances of Sr_2CrMoO_6, which is due to the ionic radius of the W^{5+} (0.62 Å) which is larger than the ionic radius of Mo^{5+} (0.61 Å). The results are consistent with our XRD refinements data.

Keywords: Double perovskites; X-ray absorption spectroscopy; EXAFS.

INTRODUCTION

In ordered double perovskites, denoted as $A_2BB'O_6$ (where A = alkaline-earth or rare-earth ion), the transition metal sites are occupied alternately by different cations B and B′. It is well known that the differences in the valence and size between B and B′ cations in double perovskite type compounds are crucial in controlling physical properties.[1-2] Recently, Kobayashi et al. have reported a high spin polarization for an oxide material with a double-perovskite structure, Sr_2FeMoO_6, which also has a high Curie temperature, (T_c = 420 K).[3] Other Fe-based ordered double perovskites A_2FeMO_6 (A = Ba, Sr, Ca; M = Mo, Re) have also been reported having a tunneling magnetoresistance (TMR) nature and a high T_c.[4-9]

In a recent report, Goodenough et al. have first reported the series of samples $(Sr_{2-x}Ca_x)FeMoO_6$ $(0 \le x \le 2)$.[10] They found that ferromagnetic long-range ordered domains are coupled antiferromagnetically across antiphase boundaries; random disorder within domains may be small. On the other hand, tunneling-type magnetoresistance has also been reported on Cr-based double perovskites A_2CrMO_6 (A = Sr, Ca; M = Mo, W, Re).[11-13] The major difference between Fe-based and Cr-based double perovskites is that in the Cr compound, there can be no valence degeneracy between the Cr and the Mo or W ions, since Cr can only be in the 3+ state ($3d^3$). Anyway, at this stage a very little research clarified the local structure by extended X-ray absorption fine structure (EXAFS). In this article, we report for the first time the Fe and Cr EXAFS spectra to investigate the local structure of $Sr_{2-x}Ca_xFeMoO_6$ $(0 \le x \le 2)$ and Sr_2CrMO_6 (M = Mo, W) compounds.

EXPERIMENTAL SECTION

The synthesis of polycrystalline samples of $(Sr_{2-x}Ca_x)FeMoO_6$ $(0 \le x \le 2.0)$ and Sr_2CrMO_6 (M = Mo, W) were reported elsewhere by our group.[14,15] X-ray absorption experiments were carried out at the National Synchrotron Radiation Research Center (NSRRC), Hsinchu, Taiwan. All data were collected at room temperature. Fe and Cr *K*-edge data were recorded in transmission mode for synthesized powder mounted on scotch tape, at the BL 17C Wiggler beam line using a double-crystal Si (111) monochromater. The X-ray harmonic was rejected by mirrors. The spectra were scanned from 5.8 to 7.5 keV using a gas-ionization detector. The ion chambers used for measuring the incident (I_0) and transmitted (I) beam intensities were filled with a mixture of N_2 and H_2 gases and a mixture of N_2 and Ar gases, respectively. The en-

Dedicated to Professor Ching-Erh Lin on the Occasion of his 66th Birthday and his Retirement from National Taiwan University

* Corresponding author. rsliu@ntu.edu.tw

ergy scales were calibrated by monitoring with Fe and Cr foils. The data analysis of the experimental EXAFS spectra was performed using the UWXAFS package.[16-17] The AUTOBK code was used for background subtraction.[18] The resulting EXAFS spectra were k^3-weighted and Fourier transformed in the range of $4 \le k \le 14$ Å^{-1} with a Hanning apodization function. A nonlinear least-square curve fitting procedure in the FEFFIT code was carried out in the range of $1.8 \le k \le 4.1$ Å^{-1}, corresponding to the first shell of M-O, where M was Fe or Cr.[19] Based on the plane wave single scattering, the general EXAFS formula can be expressed as a summation of over all shells i by the following equation.[20]

$$\chi(k) = S_0^2 \sum_i \frac{N_i F_i(k)}{kR_i^2} \sin[2kR_i + \delta_i(k)] e^{-2R_i/\lambda} e^{-2k^2\sigma_i^2}$$

where $F_i(k)$ is the backscattering amplitude from each of the N_i atoms in the shell I at distance R_i, with Debye-Waller factor σ_i^2. S_0 is the amplitude reduction factor, $\delta_i(k)$ is the total phase shift, and $\lambda(k)$ is the photoelectron mean free path. The $F_i(k)$, $\delta_i(k)$ and $\lambda(k)$ were theoretically calculated by a curved wave *ab initio* procedure in the code FEFF7.[21] The refinements were based on the minimization R factor,[22] which is defined as follows:

$$\Re = \frac{\sum_{i=1}^{N} \left\{ [\mathrm{Re}(f_i)]^2 + [\mathrm{Im}(f_i)]^2 \right\}}{\sum_{i=1}^{N} \left\{ [\mathrm{Re}(\tilde{\chi}_{data_i})]^2 + [\mathrm{Im}(\tilde{\chi}_{data_i}]^2 \right\}}$$

where $f_i = \tilde{\chi}_{datai} - \tilde{\chi}_{\mathrm{mod}\ eli}$ is the function to be minimized, $\tilde{\chi}$ is the function weighted by k^3, and N is the number of function evaluation. When fitting in R-space, $N = 2(R_{\max}\text{-}R_{\min})/\delta R$, where δR is the grid spacing in R-space.

In the fitting procedure, the interatomic distance (R_i), Debye-Waller factor (σ_i^2), and threshold energy difference (ΔE_0) were set as variables, and the coordination number for the first shell of oxygen atoms was fixed to the crystallographic value of 6 for all the samples.

RESULTS AND DISCUSSION

XRD measurement of samples was performed by using Cu Kα radiation and it is confirmed by the Rietvelt refinement method to demonstrate the samples are phase pure and in single phase.[14,15] Experimental k^3-weighted Fe K-edge EXAFS spectra of $(Sr_{2-x}Ca_x)FeMoO_6$ ($0 \le x \le 2.0$) are shown in Fig. 1, and the Fourier transforms F(R) are shown in Fig. 2. The data range taken for transformation is from 4 to 14 Å^{-1}. Structural parameters were obtained from fitting in r-space in the interval of 1.8-2.3 Å^{-1}. The solid lines and empty circles represent the fitted and experimental data, respectively. The first prominent peak in the Fourier transform is assigned to the Fe-O contribution. The bond length between atoms, Debye-Waller factor, and EXAFS fitting parameter of $(Sr_{2-x}Ca_x)FeMoO_6$ ($0 \le x \le 2.0$) samples are listed in Table 1. Our research interest is on the variation of local structure of FeO_6 octahedron arrangement, and we therefore discuss the fitting on the first peak in order to obtain the Fe-O bond distances which are indicating a higher degree of regularity of

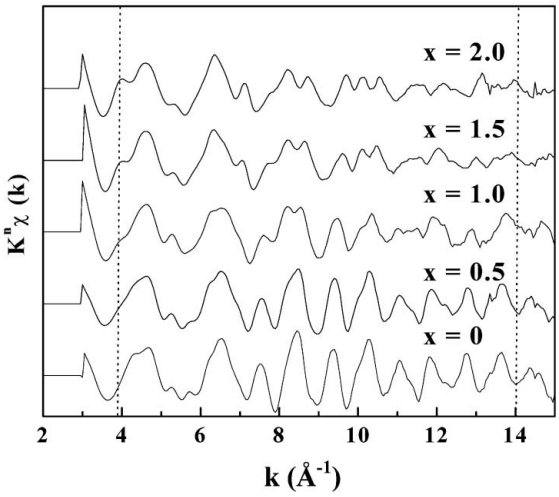

Fig. 1. Experimental k^3-weighted Fe K-edge EXAFS spectra of $(Sr_{2-x}Ca_x)FeMoO_6$ ($0 \le x \le 2.0$).

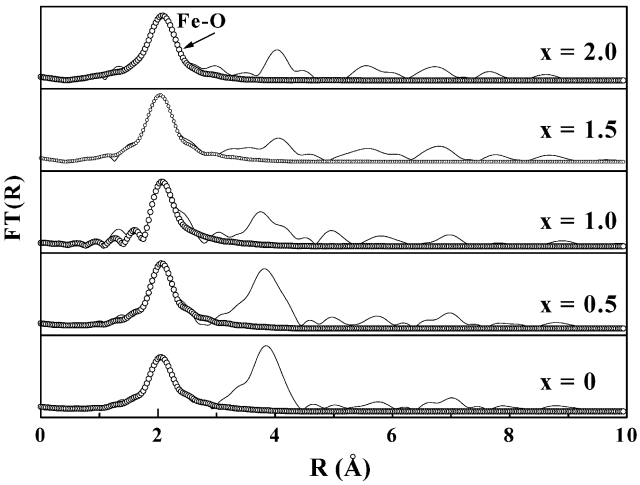

Fig. 2. Fourier transforms F(R) of the k^3-weighted Fe K-edge EXAFS spectra of $(Sr_{2-x}Ca_x)FeMoO_6$ ($0 \le x \le 2.0$). The solid line and empty circles represent the fitted and experimental data, respectively. The first prominent peak in the Fourier transform is assigned to the Fe-O contribution.

Table 1. The bond length between atoms, Debye-Waller factor, and EXAFS fitting parameter of the $(Sr_{2-x}Ca_x)FeMoO_6$ ($0 \le x \le 2.0$) samples

		x = 0	x = 0.5	x = 1.0	x = 1.5	x = 2.0
EXAFS	Fe-O(Å) (average)	1.999	1.996	1.991	2.034	2.012
EXAFS	Fe-O(1) (equatorial)	1.982	1.980	1.976	2.001	1.991
EXAFS	Fe-O(2) (axial)	2.032	2.029	2.021	2.099	2.055
σ^2	($Å^2$)	0.0045	0.0038	0.0047	0.074	0.092
R	(Å)	[1.8, 2.3]	[1.8, 2.3]	[1.8, 2.3]	[1.8, 2.3]	[1.8, 2.3]
K	($Å^{-1}$)	[4, 14]	[4, 14]	[4, 14]	[4.5, 14]	[4.5, 14]
$\Re$		3.8×10^{-4}	5.9×10^{-4}	2.7×10^{-4}	7.8×10^{-3}	9.2×10^{-3}

the FeO_6 octahedron in the double perovskites framework. Table 1 presents the EXAFS refinement results for all the samples. When x increased from 0 to 1.0, the Fe-O bond distance decreases steadily from 1.999 to 1.991. At the same time, above 1.0 the structure is transformed into monoclinic and shows a higher Fe-O bond distance (2.034) and it reduces to 2.012 when x becomes 2.0. The results are consistent with our XRD refinement data.[14] Debye-Waller factors for x = 0 ($\sigma^2 = 0.045$) and x = 2.0 ($\sigma^2 = 0.092$) are also reported in Table 1. It is noted that the Debye-Waller factor for x = 0 is notably smaller than those of x = 2, which is indicating a higher degree of regularity of the FeO_6 octahedron in the double perovskite tetragonal frameworks.

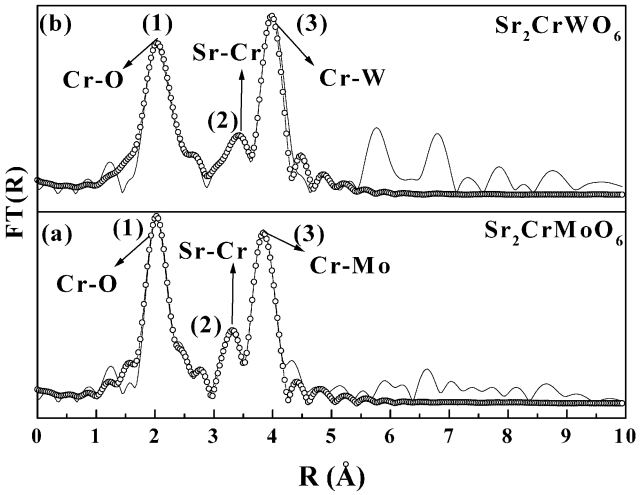

Fig. 3. Fourier transforms F(R) of the k^3-weighted Cr *K*-edge EXAFS spectra of Sr_2CrMO_6 (M = Mo, W). The first prominent peak in the Fourier transform is assigned to the Cr-O contribution. The second peak corresponds to the Sr-Cr contributions. The third peak corresponds to the Cr-Mo (Cr-W) contributions.

Fig. 3 shows the Fourier transformed F(R) EXAFS data recorded for Sr_2CrMO_6 (M = Mo, W) samples at the Cr *K*-edge. The first prominent peak in the Fourier transform is assigned to Cr-O contribution and is followed by the second peak corresponding to Sr-Cr distances. The third prominent peak is assigned to the Cr-Mo (Cr-W) distance. The bond length between atoms, Debye-Waller factor, and EXAFS fitting parameter of Sr_2CrMO_6 (M = Mo, W) samples are listed in Table 2. It is noted that the first peak of Cr-O, second peak of Sr-Cr and third peak of Cr-Mo bond distance in Sr_2CrWO_6 are all slightly larger than Sr_2CrMoO_6, which is due to the larger ionic radius of the W^{5+} (0.62 Å) compared to that of Mo^{5+} (0.61 Å).

CONCLUSIONS

We have carried out the Fe and Cr *K*-edge EXAFS analysis to study the local structure of $(Sr_{2-x}Ca_x)FeMoO_6$ ($0 \le x \le 2.0$) and Sr_2CrMO_6 (M = Mo, W) systems. The data show that the structure is transformed from a high symmetry tetragonal (x = 0) to a low symmetry monoclinic unit cell (x = 2.0). Understanding the effect of Ca^{2+} substitution on the local struc-

Table 2. The bond length between atoms, Debye-Waller factor, and EXAFS fitting parameter of the Sr_2CrMO_6 (M = Mo, W) samples

		Sr_2CrMoO_6	Sr_2CrWO_6
EXAFS	Cr-O (Å)	1.985	1.989
σ^2	($Å^2$)	0.051	0.083
R	(Å)	[1.8, 4.1]	[1.8, 4.1]
K	($Å^{-1}$)	[4.4, 14]	[4.4, 14]
EXAFS	Sr-Cr (Å)	3.399	3.405
EXAFS	Cr-Mo(W) (Å)	3.981	4.086

ture of the $(Sr_{2-x}Ca_x)FeMoO_6$ system provides important insights into how the structure of these materials can be tailored to give optimum chemical and electronic properties. Moreover, in the Sr_2CrMO_6 (M = Mo, W) system our interest is focused on double perovskite compounds having the general formula $A_2(BB')O_6$, since various B′ metal ions can be stabilized by adequately controlling structure and synthesis conditions. The EXAFS curve-fitting analysis allows us to distinguish the difference in Cr-O bond lengths for different substitutions of B′ metal ions, which supports the long-range structure presented by Rietveld refinement.

ACKNOWLEDGEMENTS

We thank for the National Science Council of Taiwan financial support under the grant number 93-2113-M-002-006 and the Ministry of Economic Affairs of Taiwan under the grant number 93-EC-17-A-08-S1-0006.

Received January 31, 2005.

REFERENCES

1. Galasso, F. *Inorg. Chem*. **1963**, *2*, 482.
2. Nakamura, T.; Choy, J. H. *J. Solid State Chem*. **1977**, *20*, 233.
3. Kobayashi, K.-I.; Kimura, T.; Sawada, H.; Terakura, K.; Tokura, Y. *Nature* **1998**, *395*, 677.
4. Maignan, A.; Raveau, B.; Martin, C.; Hervieu, M. *J. Solid State Chem*. **1999**, *59*, 11159.
5. Alonso, J. A.; Casais, M. T.; Martínze-Lope, M. J.; Velasco, P.; Muñoz, A.; Fernández-Díaz, M. T. *Chem. Mater.* **2000**, *161*, 12.
6. Borges, R. P.; Thomas, R. M.; Cullinan, C.; Coey, J. M. D.; Suryanarayan, R.; Ben-Dor, L.; Pinsard-Gaudart, L.; Revcolevschi, A. *J. Phys. Condens. Matter.* **1999**, *11*, L445.
7. Ritter, C.; Ibarra, M. R.; Morellón, L.; Blasco, J.; García, J.; De Teresa, J. M. *J. Phys. Condens. Matter.* **2000**, *12*, 8295.
8. Prellier, W.; Smolyaninova, W.; Bisbas, A.; Galley, C.; Greene, R. L.; Ramesha, K.; Gopalakrishnan, J. *J. Phys. Condens. Matter.* **2000**, *12*, 965.
9. Kobayashi, K.-I.; Kimura, T.; Sawada, H.; Terakura, K.; Tokura, Y. *Phys. Rev. B* **1999**, *59*, 11159.
10. Goodenough, J. B.; Dass, R. I. *Inter. J. Ino. Mater.* **2000**, *2*, 3.
11. Arulraj, A.; Ramesha, K.; Gopalakrishnan, J.; Rao, C. N. R. *J. Solid State Chem*. **2000**, *155*, 233.
12. Philipp, J. B.; Reisinger, D.; Schonecke, M.; Marx, A.; Erb, A.; Alff, L.; Gross, R. *Appl. Phys. Lett*. **2001**, *79*, 3654.
13. Kato, H.; Okuda, T.; Okimoto, Y.; Tomioka, Y. *Appl. Phys. Lett*. **2002**, *81*, 328.
14. Chan, T. S.; Liu, R. S.; Guo, G. Y.; Hu, S. F.; Lin, J. G.; Chen, J. M.; Attfield, J. P. *Chem. Mater.* **2003**, *15*, 425.
15. Chan, T. S.; Liu, R. S.; Guo, G. Y.; Hu, S. F.; Lin, J. G.; Lee, J. F.; Jang, L. Y.; Chang, C.-R.; Huang, C. Y. *Solid State Commun*. **2004**, *130*, 815.
16. Frenkle, A. I.; Stern, E. A.; Voronel, A.; Qian, M.; Newville, M. *Phys. Rev. B* **1993**, *48*, 12449.
17. Frenkle, A. I.; Stern, E. A.; Voronel, A.; Qian, M.; Newville, M. *Phys. Rev. B* **1993**, *49*, 11662.
18. Newville, M.; Livins, P.; Yacoby, Y.; Rehr, J. J.; Stern, E. A. *Phys. Rev. B* **1993**, *47*, 14126.
19. Newville, M.; Livins, P.; Yacoby, Y.; Rehr, J. J.; Stern, E. A. *Phys. Rev. B* **1995**, *208*, 154.
20. Sayers, D. E.; Bunker, B. A. In *X-ray Absorption: Principles Applications, Techniques of EXAFS, SEXAFS, and XANES Koningsberger*; Wiley-Interscience: New York, 1988.
21. Zabinsky, S. I.; Rehr, J. J.; Ankudinov, A.; Albers, R. C.; Eller, M. J. *Phys. Rev. B* **1995**, *52*, 2995.
22. Newville, M. *FEFFIT Document*, 1996.